Chain Force Concept in Systems of Interacting Chains

J. Gao and J. H. Weiner

Division of Engineering and Department of Physics, Brown University, Providence, Rhode Island 02912

Received February 6, 1990; Revised Manuscript Received April 1, 1990

ABSTRACT: The concept of the chain force, that is, the force that must be applied to the end atoms of a long-chain molecule in order to maintain its end-to-end distance at a fixed value, is well-defined for a system of noninteracting chains. We show here how this concept may be extended to chain systems with both intrachain and interchain noncovalent interactions and develop methods for its computation from the results of the molecular dynamics simulation of model systems. A simulation is made of a chain with fixed end atoms in interaction with a free melt of like chains with excluded-volume interactions modeled by a potential approximating hard spheres. For sufficiently long chains and sufficiently high reduced density of the system, it is found that the chain force–distance relation approaches Gaussian in accord with the Flory theorem. However, at high reduced density it is found that the chain force is due primarily to the screened excluded-volume interactions rather than to the covalent interactions as in an isolated ideal chain. For a chain in interaction with an anisotropic system of chains, as is the case in a stretched network, it is found that the chain force is no longer axial—that is, the line of action of the chain force is not parallel to the chain vector. The chain force is therefore equivalent to an axial force plus an applied moment; this moment is found to produce a significant softening effect on the stress-extension behavior.

1. Introduction

The concept of the axial force exerted by a long-chain molecule, regarded as an entropic spring, plays a central role in the classical molecular theory of rubber elasticity. It will be helpful here to recall briefly some of the essential steps in the development of that theory. The configurational entropy $S(\mathbf{R})$ of a long-chain molecule with end-to-end vector $\mathbf{R}$ is determined from the relation

$$S(\mathbf{R}) = k \log p(\mathbf{R}) \tag{1.1}$$

where $p(\mathbf{R})$ is the probability density of observing the displacement $\mathbf{R}$ in a random walk equivalent to the polymer model under consideration. The force $\mathbf{f}$ required to maintain the chain vector fixed at $\mathbf{R}$ is then

$$f_i = -T\frac{\partial S}{\partial R_i} = -kT\frac{\partial}{\partial R_i}\log p(\mathbf{R}) \tag{1.2}$$

where f_i and R_i are the components of the vectors $\mathbf{f}$ and $\mathbf{R}$ with respect to a rectangular Cartesian coordinate system x_i, $i = 1, 2, 3$.

For a sufficiently long chain that is far from fully extended and is ideal in the sense that there are no interactions between monomers that are widely separated along the chain, the probability density $p(\mathbf{R})$ is Gaussian

$$p(\mathbf{R}) = \left(\frac{3}{2\pi\langle R^2\rangle_0}\right)^{3/2}\exp[-3R^2/(2\langle R^2\rangle_0)] \tag{1.3}$$

where $R = |\mathbf{R}|$ and $\langle R^2\rangle_0$ is the mean-square end-to-end distance of the corresponding free chain. For the Gaussian chain, therefore, the force $\mathbf{f}$ required to maintain the chain vector fixed at $\mathbf{R}$ is

$$f_i = 3kTR_i/\langle R^2\rangle_0 \tag{1.4}$$

i.e., it is linear in the distance R and axial—that is, parallel to the chain vector. (For brevity, we refer to the vector f_i, etc., instead of to f_i, the components of $\mathbf{f}$.)

Consider next a network of noninteracting chains in which, for simplicity of discussion, we assume that the junctions do not undergo thermal motion. The stress in such a system can be written in the form

$$t_{ij} = \frac{1}{v}\sum_{\gamma} f_i(\gamma)R_j(\gamma) \tag{1.5}$$

where v is the volume of the system, $f_i(\gamma)$ is the force required to maintain the chain vector $R_j(\gamma)$ of chain γ, the sum is carried out over all chains of the system, and t_{ij} is the stress tensor (force per unit current area), $i, j = 1, 2, 3$. This expression for the stress may be derived, for example, by application of the principle of virtual work.[1] It may also be derived, with suitable assumptions, from thermodynamic considerations, as discussed further in section 6, eqs 6.14–6.18.

For the case of constant-volume uniaxial deformation in the x_1 direction, the affine assumption leads to

$$R_1(\gamma) = \lambda R_{01}(\gamma) \qquad R_2(\gamma) = \lambda^{-1/2}R_{02}(\gamma)$$
$$R_3(\gamma) = \lambda^{-1/2}R_{03}(\gamma) \tag{1.6}$$

where $R_{0i}(\gamma)$ are the chain vectors in the reference state. The assumptions of an isotropic reference state and Gaussian chains then lead to the classical result

$$t_{11} - t_{22} = \nu kT[R_0^2/\langle R^2\rangle_0](\lambda^2 - \lambda^{-1}) \tag{1.7}$$

where ν is the number of chain per unit volume and $[R_0^2/\langle R^2\rangle_0]$ is the average of this quantity over the network.

This derivation has said nothing about intra- or inter-noncovalent interactions. Yet it is clear that these interactions must be present and play an important role. As seen from eqs 1.4 and 1.5, consideration of the chain forces alone leads to a pressure p

$$p = -\frac{1}{3}\sum_{i=1}^{3} t_{ii} = \frac{-kT}{v}\sum_{\gamma} R^2/\langle R^2\rangle_0 \tag{1.8}$$

which is always negative for nonzero R. Therefore, in the absence of a balancing positive pressure, the system of chains must collapse to a point. The classical treatment assumes that this balancing pressure is due to the noncovalent (principally excluded volume) interactions between the atoms of the system, and it is furthermore assumed that this is the only contribution that excluded volume makes to the state of stress in rubberlike solids.

0024-9297/91/2224-5179$02.50/0

It is for this reason that the classical theory contents itself with the evaluation of the deviatoric stress in the system, that is the difference between the total stress and the mean stress. For uniaxial extension, this is equivalent to restricting attention to the stress difference $t_{11} - t_{22}$, with the understandng that the value of t_{22} will be determined from the specifications of $t_{22} = t_{33}$ on the lateral surfaces of the stretched body. From eq 1.5, the stress difference $t_{11} - t_{22}$ can be written as

$$t_{11} - t_{22} = \frac{1}{v}\sum_{\gamma}(f_1(\gamma)R_1(\gamma) - f_2(\gamma)R_2(\gamma)) \qquad (1.9)$$

Frequently the assumption $t_{22} = t_{33} = 0$ is made. It is then also convenient to rewrite eq 1.7 in terms of T_{ij}, the stress expressed as a force per unit of original area. For the deformation described by eq 1.6, $T_{11} = \lambda^{-1}t_{11}$ and eq 1.7 takes the form

$$T_{11} = \nu kT[R_0^2/\langle R^2\rangle_0](\lambda - \lambda^{-2}) \qquad (1.10)$$

Atomic View of Stress. We have been conducting the computer simulation of idealized atomistic models of rubberlike solids for the purpose of reexamining the roles of covalent and noncovalent potentials, on the level of atom–atom interactions, in the development of stress in rubberlike solids.[2-5] In most of these calculations we utilize a purely repulsive noncovalent potential, approximating a hard-sphere potential, and an important parameter, as in the theory of liquids, is the reduced density, $\rho = n\sigma^3/v$, where σ is the hard-sphere diameter and n/v is the atom number density. The physical picture presented by these simulations is in direct opposition to that underlying the classical theory.

(a) At low values of the reduced density ρ, the mean force in the covalent bonds of the system is positive, corresponding to these bonds in a state of tension. This tensile force may be traced to the "centrifugal" force required by the thermal motion of the atoms subject to the geometrical constraint of constant bond length. This tensile force in the bonds is fully in accord with the classical molecular picture of the chains exerting tensile axial forces.

However, as ρ increases, the mean force in the bonds decreases, and at values of $\rho \sim 1$ appropriate to liquids and rubberlike solids, this force is negative, corresponding to these bonds in compression—a situation incompatible with the simple picture of chains exerting tensile forces.

(b) The purely repulsive excluded-volume noncovalent interactions, examined on the level of atom–atom interactions, exhibit a complementary ρ dependence that is also counterintuitive. At very low values of ρ, the contribution of these interactions is purely hydrostatic, as assumed in the classical theory. However, as ρ increases, the excluded-volume interactions make an increasingly anisotropic or nonhydrostatic contribution to the state of stress in a deformed rubberlike solid until, at $\rho \sim 1$, the tensile stress in a stretched sample is due entirely to these interactions; in fact, the covalent contributions to the stress under these conditions is compressive.

The surprising result that a two-body purely repulsive hard-sphere potential can give rise to an anisotropic tensile stress is traced, in these simulations, to the fact that the excluded-volume interactions are screened by the covalent structure that imposes restrictions on the motion of the atoms of the system. In the reference state of the system, the covalent structure is macroscopically isotropic, and the screening leaves the excluded-volume contribution to the stress hydrostatic. However, deformation of the body causes the covalent structure and, therefore, the excluded-volume stress contribution both to become anisotropic. It should be noted that a model network of freely jointed chains with hard-sphere interactions is a purely entropic system. Therefore, the simulation results that the excluded-volume interactions, at large ρ, are responsible for the tensile stress in a stretched sample do not contradict, in any way, the well-known conclusion from experimental data that rubber elasticity is primarily entropic.[5]

In spite of the very different physical picture presented by our atomic simulations from that underlying the classical theory, the agreement of that theory with experiment is excellent, although the small discrepancy sometimes called the Mooney effect[6] still awaits a definitive microscopic explanation. It is the primary purpose of the present paper to attempt to reconcile the dominant role of excluded-volume interactions observed in our simulations on the atomic level with the success of the use of the chain force concept in the classical theory. At the same time, the changes that we observe in the chain force concept as due to excluded-volume effects in dense systems, as well as excluded-volume effects on segment orientation, may provide, at least in part, a molecular basis for the Mooney effect. The general structure of the paper and the questions it deals with are as follows:

(i) We begin, in section 2, with consideration, on the basis of equilibrium statistical mechanics, of the concept of the chain force in a system of interacting chains and give three alternate equivalent procedures for the calculation of this force.

(ii) The concept of axial force in a Gaussian chain as developed through eqs 1.1–1.4 was first developed for isolated chains with no long-range noncovalent interactions. It was initially employed in treating dense networks as a natural first step without any detailed attempt at its justification.[7] Later work based its use on what has come to be known[8] as the Flory theorem, which states[8] that, in a dense melt of long, identical chains with excluded-volume interactions, the probability distribution $p(\mathbf{R})$ for any individual chain is again Gaussian. This result has been examined theoretically,[8,10,11] by computer simulation,[12-14] and experiment[15] and is now regarded as well based. We return to the Flory theorem in section 3 and by computer simulation reexamine its implications in regard to the nature of the forces acting on a chain in such a dense melt, with particular attention to the role of covalent and noncovalent (excluded volume) interactions in the generation of this force.

(iii) The Flory theorem applies to a free melt, i.e., to a melt with no geometrical constraints placed on the chain vectors. Such a system is always macroscopically isotropic. In a network, the collection of chain vectors is isotropic only in the reference state. When the system is deformed, the system of chain vectors becomes anisotropic. How does this anisotropy affect the Flory theorem? Is it possible to define a chain force in such a strongly interacting system so that eq 1.5 remains valid? These questions are treated through the simulation of a model system in section 4.

(iv) The results of these simulations show the important influence of excluded-volume interactions on segment orientation in a deformed network. This is in accord with previous theoretical analyses,[16-18] simulations,[5,19] and experiment.[20,21] The simulations in section 4 also demonstrate the important effect of segment orientation on chain force. Of necessity these molecular dynamics simulations are for systems of short chains. In section 5 we continue an examination of this effect for long chains by means of Monte Carlo calculations, and in section 6 an

analytical stress–strain relation based on the insights obtained from the computer simulations is developed.

(v) The final section 7 contains a summary and conclusions.

2. Chain Force with Interchain Interactions

Chain Model. Although much of what we say in this section applies directly or is easily generalized to more realistic models, we present the discussion in terms of a chain model that we have employed in several of our previous simulations.[2,4,5] It approximates the hard-sphere, freely jointed chain and is the simplest chain model that has both the covalent bonding characteristic of macromolecules and the attribute of excluded volume. For computational and conceptual convenience the covalent potential is represented by a stiff linear spring and the hard-sphere potential is replaced by the repulsive part of the Lennard-Jones potential. That is, the covalent potential $u_c(r)$ is

$$u_c(r) = \frac{1}{2}\kappa(r - a)^2 \tag{2.1}$$

where r is the distance between adjacent atoms on a given chain and the noncovalent potential is

$$\begin{aligned} u_{nc}(r) &= 4\epsilon[(\sigma/r)^{12} - (\sigma/r)^6] \quad \text{for } r \leq r_0 \\ &= u_{nc}(r_0) \quad \text{for } r \geq r_0 \end{aligned} \tag{2.2}$$

where r denotes the distance between any pair of atoms on a given chain or between any pair of atoms on different chains and $r_0 = 2^{1/6}\sigma$.

Tethered Chain. Consider next a chain with N bonds with atom positions $\mathbf{x}_m$, $m = 0, ..., N$, with atoms 0 and N fixed in space and $\mathbf{x}_N - \mathbf{x}_0 = \mathbf{R}$. The remaining atoms of the chain, $m = 1, ..., N - 1$, are free to undergo thermal motion. We refer to this chain as the tethered chain. In addition to the intrachain covalent and noncovalent interactions, all of the atoms of the tethered chain are in noncovalent interaction with a collection of surrounding chains; these surrounding chains may be in the state of a free melt or a network.

Since we are using flexible models[22] for the chains, rectangular Cartesian coordinates may be employed and attention confined to the configurational portion of the partition function

$$Z(\mathbf{R},T) = \int_{r_{xy}} e^{-\beta V(\mathbf{x},\mathbf{y};\mathbf{R})}\, d\mathbf{x}\, d\mathbf{y} \tag{2.3}$$

where $\mathbf{x} = \{\mathbf{x}_1, ..., \mathbf{x}_{N-1}\}$ and $\mathbf{y}$ denotes the coordinates of the atoms of the collection of surrounding chains that are free to undergo thermal motion. Then the forces $\mathbf{f}$ and $-\mathbf{f}$ that must be applied to the fixed end atoms of the tethered chain (atoms $m = N$ and $m = 0$, respectively) are obtained from the expression

$$f_i = \frac{1}{Z}\int \frac{\partial V}{\partial R_i} e^{-\beta V}\, d\mathbf{x}\, d\mathbf{y} = -kT\frac{\partial}{\partial R_i}\log Z(\mathbf{R},T) \tag{2.4}$$

It is seen that the external force $\mathbf{f}$ is that necessary to balance the time average of all the interchain and intrachain forces acting on atom N, with an analogous statement applying to $-\mathbf{f}$ and atom 0.

Virial Force Expression. We set $\mathbf{x}_0 = 0$ and $\mathbf{x}_N = \mathbf{R}$ and write $V(\mathbf{x},\mathbf{y};\mathbf{R})$ in greater detail as

$$V(\mathbf{x},\mathbf{y};\mathbf{R}) = \sum_{m=1}^{N} u_c(r_m) + \sum_{\alpha\in nc} u_{nc}(r_\alpha) + V_{-1}(\mathbf{y}) \tag{2.5}$$

where $\mathbf{r}_m = \mathbf{x}_m - \mathbf{x}_{m-1}$; $\mathbf{r}_\alpha = \mathbf{x}_m - \mathbf{x}_{m'}$ and where $m, m' = 0, 1, ..., N$ when α represents a pair of atoms on the tethered chain, $\mathbf{r}_\alpha = \mathbf{x}_m - \mathbf{y}_p$, when α represents a pair of atoms with one on the tethered chain and the second in the surrounding chain system, the notation $a\in nc$ denotes a sum over all pairs with at least one atom on the tethered chain in noncovalent interaction, $V_{-1}(\mathbf{y})$ is the total energy of the interactions that do not involve any atom of the tethered chain, and $r = |\mathbf{r}|$. Note that $\mathbf{R}$ appears in $V(\mathbf{x},\mathbf{y};\mathbf{R})$ through the term $u_c(r_N)$, and the terms $u_{nc}(r_\alpha)$ in which the fixed atom at $\mathbf{x}_N = \mathbf{R}$ is one of the pair α.

Let x_{mi}, $i = 1, 2, 3$ be the components of $\mathbf{x}_m$, etc. We introduce[23] the following change of variable for the integration in the partition function, eq 2.3:

$$\begin{aligned} x_{m1} = R_1\bar{x}_{m1} \qquad x_{m2} = R_2\bar{x}_{m2} \qquad x_{m3} = R_3\bar{x}_{m3} \\ m = 1, ..., N-1 \end{aligned} \tag{2.6}$$

and define $\bar{x}_{Ni} = 1$, $i = 1, 2, 3$. Then $r_{mi} = R_i\bar{r}_{mi}$, $m = 1, ..., N$, where the summation convention is not employed in this section, $r_{\alpha i} = R_i\bar{r}_{\alpha i}$ when both atoms in pair α belong to the tethered chain, but $r_{\alpha i} = R_i\bar{x}_{mi} - y_{pi}$ when pair α includes an atom p from the surrounding chain system. The partition function then takes the form

$$Z(\mathbf{R},T) = \int_{r_{xy}} e^{-\beta V(\mathbf{x},\mathbf{y};\mathbf{R})}(R_1R_2R_3)^{N-1}\, d\bar{\mathbf{x}}\, d\mathbf{y} \tag{2.7}$$

After performing the differentiation indicated in eq 2.4, we return to the original variables. The final result for $\mathbf{f}$ is

$$\begin{aligned} f_iR_i = -(N-1)kT + \sum_{m=1}^{N}\langle r_{mi}^2 r_m^{-1} u'_c(r_m)\rangle + \\ \sum_{\alpha\in intra}\langle r_{\alpha i}^2 r_\alpha^{-1} u'_{nc}(r_\alpha)\rangle + \sum_{\alpha\in inter}\langle x_{m_\alpha i} r_{\alpha i} r_\alpha^{-1} u'_{nc}(r_\alpha)\rangle \end{aligned} \tag{2.8}$$

where $\alpha\in intra$ indicates a sum over all pairs on the tethered chain, and $\alpha\in inter$ indicates a sum over pairs α with one atom, m_α, on the tethered chain and the second in the surrounding system; carats denote time averages. We may introduce the notations

$$f_{mi} = u'_c(r_m) r_{mi} r_m^{-1} \qquad f_{\alpha i} = u'_{nc}(r_\alpha) r_{\alpha i} r_\alpha^{-1} \tag{2.9}$$

for the forces due to the covalent and noncovalent interactions and rewrite eq 2.8 as

$$\begin{aligned} f_iR_i = -(N-1)kT + \sum_{m=1}^{N}\langle f_{mi} r_{mi}\rangle + \sum_{\alpha\in intra}\langle f_{\alpha i} r_{\alpha i}\rangle + \\ \sum_{\alpha\in inter}\langle f_{\alpha i} x_{m_\alpha i}\rangle \end{aligned} \tag{2.10}$$

The procedure we have followed in arriving at eq 2.8 is analogous to that followed in ref 23 for the force on a chain in the absence of noncovalent interactions. In that reference, an interpretation of the physical significance of the virial expression for the force on a chain molecule was presented; this interpretation may be generalized readily to the present case. In the presence of chain–chain interactions, the virial expression for the chain force, eq 2.8, is important in that it expresses this force in terms of interactions with atoms all along the length of the chain whereas the direct expression of the chain force given in eq 2.4 involves only interactions experienced by the end atoms of the tethered chain. It might be thought from the latter formulation that, in the presence of chain–chain interaction, the chain force is particularly sensitive to the environment in which the chain end atoms find themselves. The virial formulation shows that this is not the case.

Probability Interpretation. By the same analysis followed for an isolated chain molecule,[24] we may show in

Table I
Chain Dimensions in Free Melt[a]

	N				
	10	15	20	25	30
$\langle R^2\rangle_0/a^2$	15.1	23.4	32.1	41.1	49.3
$C_N = (\langle R^2\rangle_0/Na^2)^{1/2}$	1.23	1.25	1.27	1.28	1.28

[a] $\rho = 0.8$, $\mu = 48$.

the present case that

$$Z(\mathbf{R},T) = Cp(\mathbf{R},T) \tag{2.11}$$

where $Z(\mathbf{R},T)$ is the partition function for the tethered chain with $\mathbf{x}_0 = 0$ and $\mathbf{x}_N = \mathbf{R}$ as defined in eq 2.3, and $p(\mathbf{R},T)$ is the probability density of finding atom N at $\mathbf{R}$ when that atom is free to undergo thermal motion; C is a constant independent of $\mathbf{R}$. It follows that, in place of eq 2.4, we may also compute $\mathbf{f}$ by the relation

$$f_i = -kT\frac{\partial}{\partial R_i}\log p(\mathbf{R},T) \tag{2.12}$$

3. Chain Forces in a Free Melt

Simulation of Melt. We employ in this and the following section the chain model described in the previous section with $\sigma = a$, $\kappa a^2/kT = 200$, and $\epsilon/kT = 0.75$. For the second parameter value, the bond length undergoes only small fractional changes, and for the third, σ may be regarded as an effective hard-sphere diameter.

The simulated polymer melt of these chains contain μ chains, each with N bonds in a basic cubic cell of edge c and volume v leading to a reduced density

$$\rho = \mu(N+1)\sigma^3/v \tag{3.1}$$

Periodic boundary conditions are employed as in our previous simulations; further details of the molecular dynamics procedure followed may be found in ref 13.

We have performed simulations for various values of N between 10 and 30, all at $\rho = 0.8$. The results for $\langle(R^2)\rangle_0$ are shown in Table I. Kremer and Grest[14] have performed simulations of polymer melts, using a chain model only slightly different from ours, with values of N as high as 400 at $\rho = 0.85$. They found, for sufficiently large N, that $\langle R^2(N)\rangle_0 = C_\infty N$ (in our notation) with the limiting characteristic ratio[25] $C_\infty = 1.32 \pm 0.02$. While our simulations do not cover sufficiently large values of N to determine the limiting value of the scaling experiment, they do yield the ratio $(\langle R^2\rangle_0/N)^{1/2} = 1.28$ in reasonably good agreement, particularly in view of the slight difference in models,[26] with the Kremer and Grest result.

In other words, although for sufficiently large ρ and N, the chains in the melt approach ideal behavior in the sense that $\langle R^2(N)\rangle_0 = C_\infty N$, the fact that $C_\infty > 1$ indicates that they do not behave as freely jointed chains with no correlation in orientation between successive links. Rather the excluded-volume interaction has the effect of limiting the possible range of angles between successive links and gives rise to a local correlation. To verify this effect, our program computes the value of

$$(N-j)^{-1}\sum_{m=1}^{N-j}\langle \mathbf{r}_m\cdot\mathbf{r}_{m+j}\rangle = \langle\langle \mathbf{r}_p\cdot\mathbf{r}_{p+j}\rangle\rangle \tag{3.2}$$

A typical result is shown in Figure 1, where it is seen that the correlation does not vanish until $j \simeq 7$.

Force on Tethered Chain. We next consider a single chain with fixed end atoms and chain vector $\mathbf{R}$ immersed in and interacting with a melt of like chains. We wish to determine the time-averaged external forces $\mathbf{f}$ and $-\mathbf{f}$ that must be applied to the fixed end atoms of the tethered chain in order to maintain their given positions. In accord with the discussion of section 2, we use three alternate procedures for computing these forces.

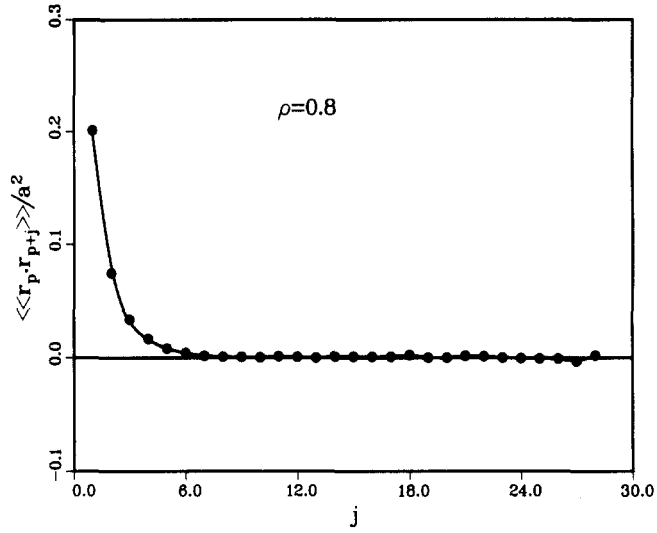

Figure 1. Intrachain segment–segment correlation, $\langle\langle \mathbf{r}_p\cdot\mathbf{r}_{p+j}\rangle\rangle$, as defined in eq 3.2, for chains in dense melt. $\mu = 48$ chains per basic cell; $N = 30$ bonds per chain; cell is cubic with edge $c = 12.3a$ and $v = 1860a^3$, leading to a reduced density $\rho = 0.8$ by eq 3.1, since $\sigma = a$ throughout.

(i) In the most direct approach, we perform a molecular dynamics simulation of the system of a single tethered chain immersed in melt of like chains. In the simulation program we determine the time average of the internal forces exerted on the end atoms of the tethered chain. The required external forces are then the negative of the computed internal forces. This direct method permits the decomposition

$$\mathbf{f} = \mathbf{f}_c + \mathbf{f}_{\text{nc-inter}} + \mathbf{f}_{\text{nc-intra}} \tag{3.3}$$

where $\mathbf{f}_c$ is the force required to balance that exerted by the covalent bond on the end atom, $\mathbf{f}_{\text{nc-intra}}$ balances that exerted by noncovalent, excluded-volume interactions between free atoms of the tethered chain on the fixed end atoms, and $\mathbf{f}_{\text{nc-inter}}$ balances the noncovalent forces exerted by melt atoms on the fixed atoms.

(ii) From a simulation of a single tethered chain in a melt we may also compute the internal forces on the end atoms by using the virial formulation of the force, eq 2.10. This yields $\mathbf{f}$ in terms of time averages over all of the mobile atoms of the tethered chain. Since it involves time averages for a larger set of atoms, it yields statistically more accurate results than method i, which involves time averages only over the fixed atoms. However, it does not permit the decomposition contained in eq 3.3.

(iii) As an indirect approach to the problem, we perform a molecular dynamics simulation of a melt of like chains with no tethered chain. The program keeps track of the chain vectors $\mathbf{R}(t)$ for all of the chains of the system at each instant of time and sorting of these vectors leads to $p(\mathbf{R})$ for this system. Then, as shown in the section 2, the required force $\mathbf{f}(\mathbf{R})$ for a tethered chain in the melt can be determined from eq 2.12. This method is computationally most efficient since it involves averages over all of the chains and one simulation leads to the relation $\mathbf{f}(\mathbf{R})$ for all $\mathbf{R}$ simultaneously.

Results. We first present the results of simulations according to method i with particular attention to the decomposition of eq 3.3 for various values of reduced density ρ. All of the simulations are performed with $\mu =$

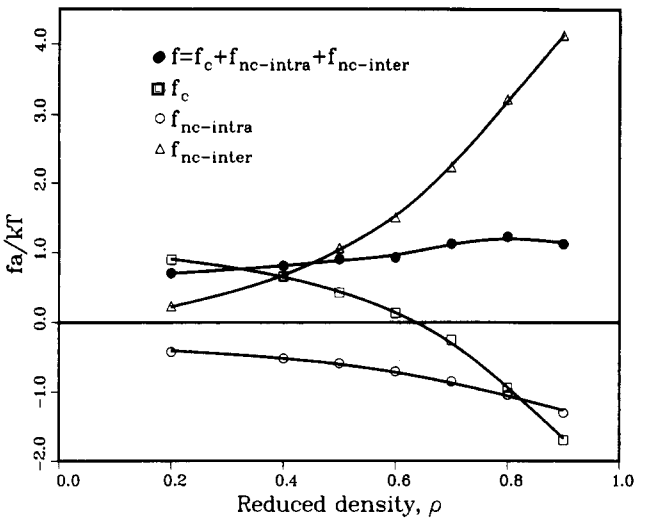

Figure 2. Force **f** required to keep end atoms of tethered chain fixed when in interaction with a free melt of like chains, together with decomposition as in eq 3.3. $N = 10$; $\mu = 48$ chains total, with one tethered; $R/Na = 0.5$ where R is end-to-end distance of tethered chain.

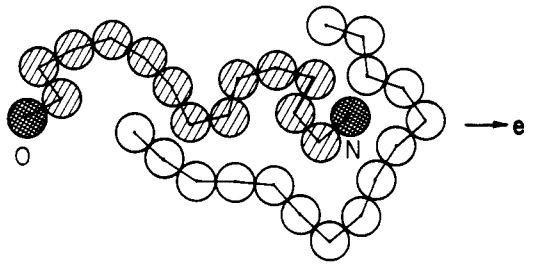

Figure 3. Schematic representation of the screening of fixed end atoms (⊗) 0 and N of tethered chain by mobile atoms (⊘) of tethered chain from interaction with atoms (O) of chains of surrounding melt. Note that excluded-volume interactions between atom N of tethered chain and atoms of melt occur more frequently in $-\mathbf{e}$ direction than in $\mathbf{e}$ direction. Intrachain excluded-volume interactions are less frequent than interchain excluded-volume interactions because of fixed value of chain vector.

48 and $N = 10$. The reduced density ρ is varied by change of basic cell volume v. The results, Figure 2, show the decomposition of **f** according to eq 3.3 At low values of ρ, the magnitude of $\mathbf{f}_{\text{nc-inter}}$ is small and the covalent contribution to the tensile force exerted by the chain is dominant, in accord with the usual physical picture. However, as ρ increases, the covalent contribution $\mathbf{f}_c$ decreases and eventually becomes negative, and it is $\mathbf{f}_{\text{nc-inter}}$ that is primarily responsible for the tensile force.

The description of an entropic spring in the presence of intrachain and interchain excluded-volume interactions that emerges from these simulations is therefore as follows: We have confined attention here to a sufficiently large value of R/Na ($R/Na = 0.5$) so that the chain is in tension[27] at all values of ρ; i.e., the fixed end atoms are subject to resultant internal forces directed toward the interior of the chain. At low values of ρ, the fixed end atoms are *pulled* inward by the covalent bonds of the chain attached to them. They are pushed outward to some degree by the intrachain excluded-volume forces, but it is the inward covalent pull that is responsible for the tension in the chain; this is in accord with the usual physical picture. At high values of ρ, however, the covalent bonds are in compression and the end atoms are *pushed* inward by the interchain noncovalent excluded-volume interactions. This occurs because these interactions in the outward direction are screened and diminished by the presence of the atoms of the chain. This screening is shown schematically in Figure 3.

Table II
Chain Force, fa/kT, on Tethered Chain Immersed in Free Melt[a]

	ρ						
	0.2	0.4	0.5	0.6	0.7	0.8	0.9
fa/kT[b]	0.70	0.81	0.90	0.94	1.13	1.23	1.12
fa/kT[c]	0.70	0.81	0.87	0.93	1.12	1.21	1.13

[a] $N = 10, R/Na = 0.5, \mu = 48$. [b] Computed from simulation as time average of resultant of all forces acting on end atoms. [c] Computed from forces acting on all atoms of chain, by means of virial expression for chain force, eq 2.10.

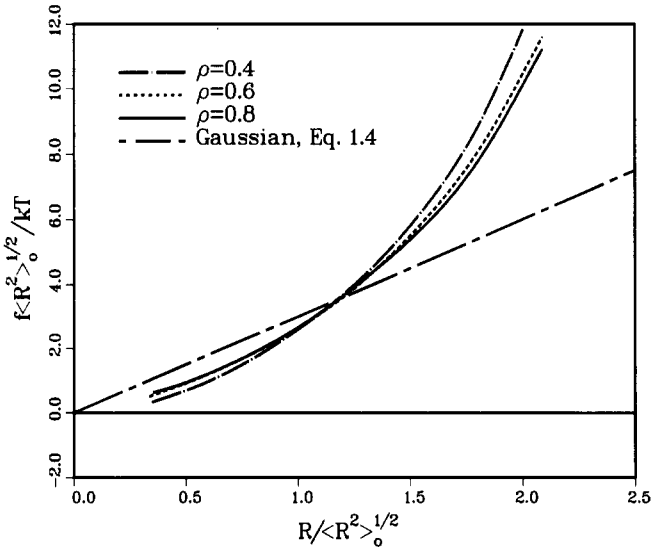

Figure 4. Chain force $\mathbf{f}(R)$ for a tethered chain with end-to-end distance R surrounded by a free melt as computed from the probability distribution $p(R)$ by use of eq 2.12 for three values of the reduced density ρ. The value of $\langle R^2\rangle_0$ used to render the simulation results nondimensional is that appropriate to each value of ρ. $N = 20$ and the reduced density ρ is varied by change of the basic cell volume v.

The results of computing the total chain force **f** by means of method ii, that is, on the basis of eq 2.10, are compared in Table II with the direct method i. It is clear that the two methods are in good agreement.

Flory Theorem. We turn next to the computation of the chain force **f** by method iii, that is on the basis of the probability distribution $p(\mathbf{R})$. Since the Flory theorem states that this distribution should approach its ideal form for sufficiently dense melts of sufficiently long chains, we would expect to find that the force law, under these conditions, approaches that for Gaussian chains, eq 1.4.

We consider first the effect of variation of the reduced density ρ. Shown in Figure 4 are the results for $f(R)$ obtained from the numerical differentiation of $p(R)$ based on melt simulations for $\rho = 0.4, 0.6$, and 0.8. It is seen that the results appear to have converged to a stable $f(R)$ relationship at $\rho = 0.8$, but that this force law is still far from Gaussian.

We turn next to the effect of N on this convergence. Unfortunately, the time constants of the system motion increase rapidly with N, and it is not possible to obtain values for $p(R)$ that are sufficiently accurate for numerical differentiation for $N > 30$. Results for $\rho = 0.8$ and $N = 10, 20$, and 30 are shown in Figure 5. The increased scatter seen in the results for large and small R is a result of fewer data available for sorting to obtain $p(R)$ in those regions. Shown also in Figure 5a are the results for the chain force as computed by the direct method i for three particular

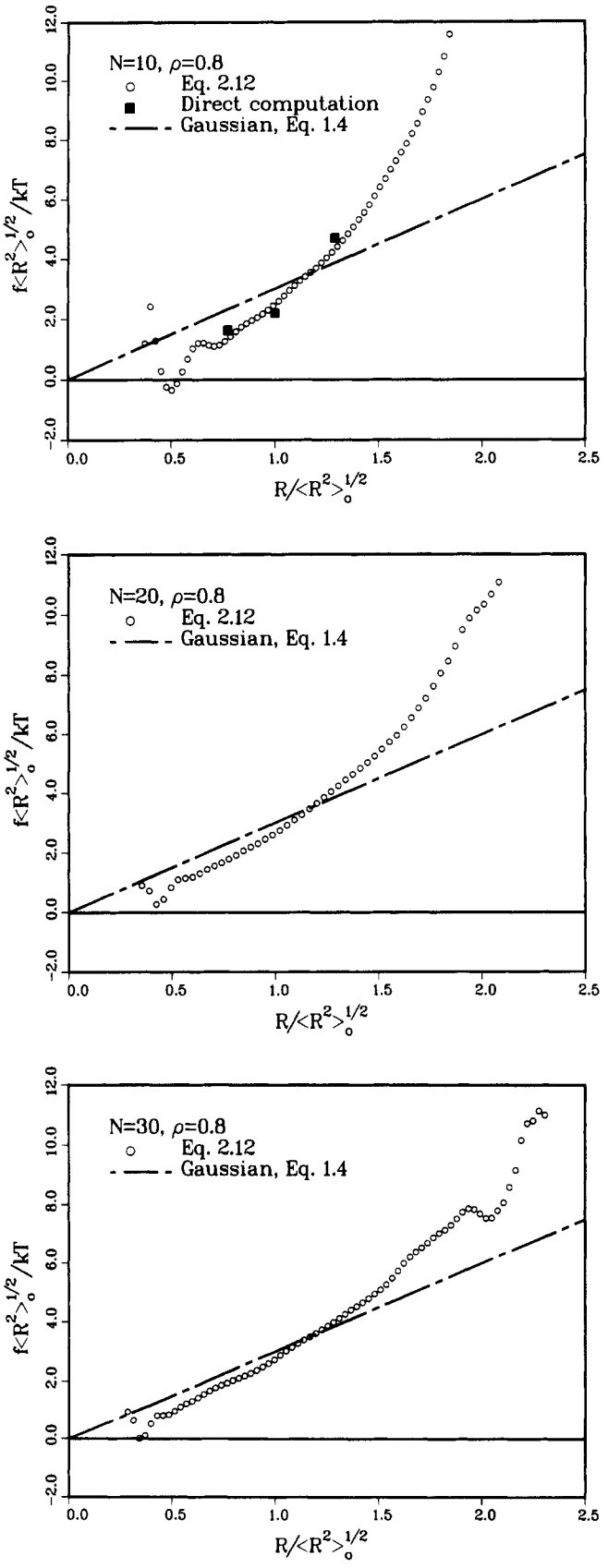

Figure 5. Approach of chain force $\mathbf{f}(R)$ to Gaussian law, eq 1.4, as the number of bonds N increases for a tethered chain surrounded by a dense free melt. Data points O are results of numerical differentiation of distribution $p(R)$ determined in simulation. Data points ■ in (a) are results of direct calculation of forces acting on end atoms of tethered chain. From top to bottom: (a) $N = 10$, (b) $N = 20$, and (c) $N = 30$, all for reduced density $\rho = 0.8$.

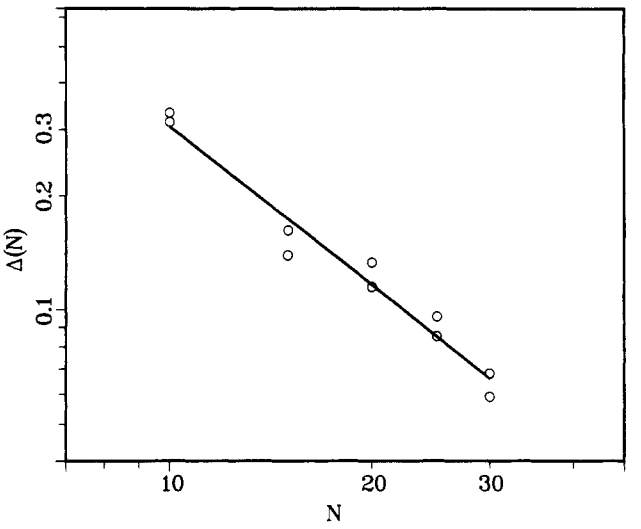

Figure 6. Approach of $f(R)$ to Gaussian as N increases, as measured by $\Delta(N)$, eq 3.4, for same system as in Figure 5. Data points shown for each value of N are for two independent simulations. Straight line is a least-squares fit to all of the data.

values of R; it is seen that they are in good agreement with those obtained by the indirect procedure of method iii.

The approach of the $f(R)$ relation toward the Gaussian relation with increasing N is seen clearly in Figure 5. As a measure of the departure of the $f(R)$ relation from Gaussian, we use the mean-square deviation over the range $0.75 \leq R/\langle R_0^2\rangle^{1/2} \leq 1.25$

$$\Delta = 2\int_{0.75}^{1.25}\left(\frac{f(R)\langle R^2\rangle_0^{1/2}}{kT} - \frac{3R}{\langle R^2\rangle_0^{1/2}}\right)^2 \mathrm{d}\left(\frac{R}{\langle R^2\rangle_0^{1/2}}\right) \quad (3.4)$$

where Δ is determined numerically from the computed values of $f(R)$. The variation of Δ with N is shown in Figure 6. We see that the simulations indicate a dependence of the form $\Delta(N) = CN^{-1.4}$, in support of the Flory theorem in the sense that $\lim_{N\to\infty}\Delta = 0$.

Estimation of Errors in Simulation. Our principal method for the estimation of error size in the results of the simulations reported in this section and in those following involved repeat calculations for selected cases with independent initial configuration and initial atomic velocity choices. For some of the results reported in the figures and tables, results from repeated runs are given as examples. Error bars are not shown; in general we estimate them to be of the order of magnitude of the symbol size or smaller.

4. Stresses and Chain Forces in an Oriented Melt

In the previous two sections we have presented a definition of the chain force that is valid in the presence of chain–chain interactions and have developed methods for its computation. We now consider the conjecture that chain force defined in this way may be used, by means of eq 1.5, to compute the deviatoric stress in networks of interacting chains.

Oriented Melt. As in ref 5 we find it advantageous to utilize a model for a polymer network that we have termed an oriented melt. To motivate this model, consider a network with fixed junctions, i.e., one in which the junctions do not undergo thermal fluctuations. Let $\mathbf{R}_0(\gamma)$ be the end-to-end vector, or chain vector, of the γ chain in the reference network configuration and $\mathbf{R}(\gamma)$ the corresponding chain vector in the deformed configuration. It is convenient in the following discussions to regard each junction as made up of a set of fixed atoms, one for each

of the chains attached to that junction. In the deformed configuration we denote the positions of the two fixed atoms for the γ chain as $\mathbf{x}^+(\gamma)$ and $\mathbf{x}^-(\gamma)$ so that $\mathbf{R}(\gamma) = \mathbf{x}^+(\gamma) - \mathbf{x}^-(\gamma)$.

We now modify this model of a network by freeing the chain end atoms at each junction and permitting the chain end atoms also to undergo thermal motion with the proviso, however, that each chain vector remains constant, representing the same chain displacement as in the network. We refer to the resulting model as an oriented melt and impose a macroscopic deformation on it as on the corresponding network: the chain vector $\mathbf{R}_0(\gamma)$ in the reference configuration is transformed into the vector $\mathbf{R}(\gamma)$ in the deformed configuration by the same affine deformation that characterizes the macroscopic deformation.

Our primary purpose in freeing the chains of the network to form the oriented melt is to increase atomic mobility and decrease relaxation times. However, a second purpose is served as well. In a real network there will be many chains with the same, or essentially the same, end-to-end vector. Each of these will be in interaction with a somewhat different environment composed of chains of different lengths and orientations. We may then regard the time-averaged behavior of a particular chain of the oriented melt as representing an ensemble average of the set of chains in a large network that all have the same chain vector. Further discussion of the oriented melt model and its computer simulation by the method of molecular dynamics may be found in ref 5. As in that reference we consider here an oriented melt in which, in the reference configuration, the chain vectors have all the same length R_0 and the chain vector directions are randomly generated corresponding to uniform probability on the unit sphere. Except as noted, there are 48 chains in the basic cell. The common length of all of the chains in the reference configuration is taken as $R_0 = \langle R^2 \rangle_0^{1/2}$, where the latter quantity is determined from simulations of the free melt with the same values of ρ and N. The model is subjected to a constant-volume uniaxial deformation with extension ratio λ in the x_1 direction.

Stress Calculations. The stress differences $t_{11} - t_{22}$ for various values of λ are computed in terms of suitable time averages from the simulation results by means of two procedures: (a) The first uses the atomic level virial stress formula,[23] namely

$$vt_{ij} = -n_t kT\delta_{ij} + \sum_{\alpha \in c} \langle r_\alpha^{-1} u'_c(r_\alpha) r_{\alpha i} r_{\alpha j} \rangle + \sum_{\alpha \in nc} \langle r_\alpha^{-1} u'_{nc}(r_\alpha) r_{\alpha i} r_{\alpha j} \rangle \quad (4.1)$$

where, in addition to previously defined quantities, n_t is the number of atoms in the basic cell free to undergo thermal motion. This approach is rigorously correct and is numerically most reliable since it involves time averages over all of the atoms of the system. (b) The chain force $\mathbf{f}(\gamma)$ acting on chain γ is determined for each chain by the direct approach of computing the resultant forces acting on its end atoms. The forces are then used in eq 1.9 to determine the stress difference $t_{11} - t_{22}$. A graphical representation of the results, expressed in terms of the stress tensor T_{11} (defined before eq 1.10), is shown in Figure 7. The numerical results for the two methods are given in Table III. It is seen that the two methods are in good agreement, thus lending support to the conjecture that the deviatoric stress may be computed in terms of the chain force as defined in section 2. Also shown in Table III, column c, are the results, for selected runs, of computing the stress by the force-based formula with the chain force

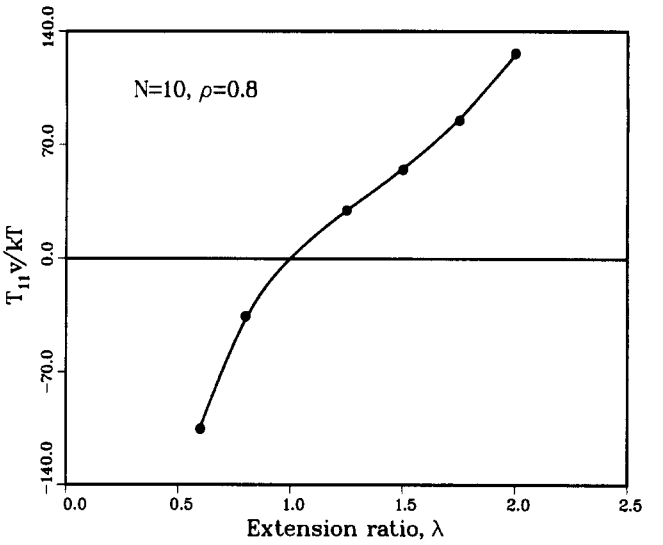

Figure 7. Stress–strain relation determined by molecular dynamics simulation for oriented melt. Stress tensor T_{11} denotes force per undeformed area. Data points are based on evaluation of simulation time averages using atomic level virial stress formula, eq 4.1. $\mu = 48$ chains in basic cell.

Table III
Stress Differences for Deformed Oriented Melt[a]

	$(t_{11} - t_{22})v/kT$			
λ	a	b	c	d
		$N = 10, \mu = 48$		
0.6	-63.2	-66.0		-66.7
0.8	-25.7	-28.7		-29.8
0.8	-28.4	-27.2	-27.7	-27.9
1.25	36.9	35.6	35.6	37.8
1.5	82.2	83.3		86.5
1.75	150.4	151.7		157.2
2.0	253.0	252.9		266.9
2.0	255.5	254.9	255.3	266.0
		$N = 10, \mu = 96$		
2.0	509.1	508.1		529.7
		$N = 20, \mu = 48$		
1.5	76.4	72.1		81.6
2.0	197.2	194.9		201.8
2.0	198.2	195.7	197.8	205.6

[a] $\rho = 0.8$. The stress difference $(t_{11} - t_{22})v/kT$ is computed by means of the following: (a) virial expression, eq. 4.1; (b) force-based formula, eq. 1.9, with chain force determined in simulation as time average of forces exerted on end atoms; (c) force-based formula, eq. 1.9, with chain force determined in simulation from eq. 2.10; (d) force-based formula, eq. 1.9, with only axial component, f_R, used.

determined in the simulation by means of the virial expression of eq 2.10; it is seen that these results agree well with those in column b in which the end-atom chain force calculation is used. One simulation reported in Table III involves $\mu = 96$ chains per basic cell instead of the usual $\mu = 48$. This simulation was undertaken to verify that the cell size used for the $\mu = 48$ simulations was adequate. Since the reduced density $\rho = 0.8$ for both cases, the cell volume v (96 chains) = $2v$ (48 chains) and it is seen that, in fact, the value of $(t_{11} - t_{22})v/kT$ for $\mu = 96$ is essentially twice that for $\mu = 48$.

Nonaxial Chain Force. In the deformed oriented melt, the distribution of chain vectors is no longer isotropic. In our previous simulations of this model, we found[5] that a consequence of this fact was that the chain vector was not a principal axis of the chain stress. This result suggests that we examine the axiality of the chain force in the deformed configuration. The simulation results do not permit an accurate determination on an individual chain

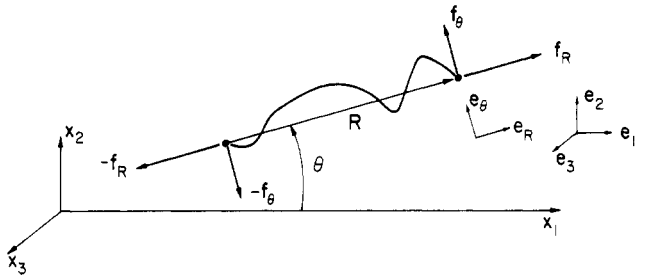

Figure 8. Schematic representation of the force acting on a chain in a stretched network when the chain vector **R** makes an angle θ with the stretch axis x_1. Shown are f_R and f_θ, the axial and transverse components of the chain force **f**; see eqs 4.6 and 4.7.

basis; since each chain is different in length and orientation in the deformed configuration, averaging over the chain forces is not possible and there is too much scatter in the numerical values of the individual force components. However, we can draw an indirect conclusion by calculating the stress on the basis of eq 1.9 using only the axial component, f_R, of each force $\mathbf{f}(\gamma)$. This method reduces the effect of numerical scatter in the individual force components since it involves a sum over all of the chains of the system. The results are shown in Table III, column d; although the differences are small, they show clearly that use of only the axial components of the chain forces leads to stresses whose absolute values are consistently too large. We conclude, therefore, that the anisotropy of chain vector distribution in a deformed oriented melt leads to chain forces that are not axial—that is, the line of action of the chain force does not coincide with the chain vector. We may represent the chain force in this case as an axial chain force plus a pair of equal and opposite forces acting perpendicularly to the chain axis and therefore exerting a moment upon the chain, Figure 8. Note that because it was only possible to simulate accurately by molecular dynamics oriented melts with short chains, the possible range of extension was restricted to $\lambda \leq 2$, and as a result, the softening observed in these simulations was small. The simulation results indicate that these chain moments have, in tension, a softening effect. In order to understand further the origin of the chain moments, we turn next to a discussion of segment and chain vector orientation of a free chain in a deformed oriented melt.

Segment Orientation. The simulation program computes the segment orientation measure

$$\langle P_2\rangle_S = \frac{1}{2}(3\langle\cos^2\theta_S\rangle - 1) \tag{4.2}$$

where θ_S is the angle between the segment and the stretch direction, with the average carried out over time and all segments of the oriented melt. The result, for various values of the extension ratio λ, are shown in Figure 9, where it may be compared with the result[28] for a network of noninteracting Gaussian chains

$$\langle P_2\rangle_S = \frac{1}{5N}(\lambda^2 - \lambda^{-1}) \tag{4.3}$$

Also shown in this figure is the segment orientation of a single free chain immersed in and interacting with the deformed oriented melt. The results show clearly that the free chain acquires, through interaction with its environment, a segment orientation that increases with λ, as does the segment orientation of the chains in the oriented melt that have their chain vectors controlled by the imposed deformation. These simulation results are therefore in qualitative accord with those obtained by Sotta et al.[21] using ^{2}H NMR on free molecules in deformed

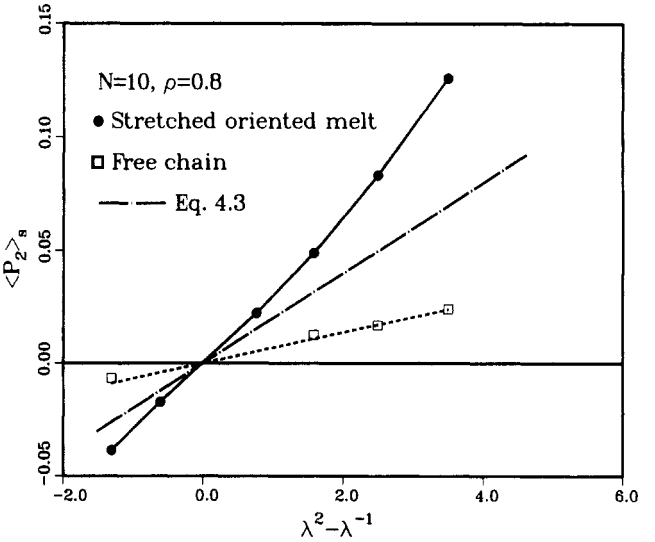

Figure 9. Segment orientation $\langle P_2\rangle_S$ for chains of stretched oriented melt and for free chain in interaction with this oriented melt. Also shown is the theoretical result for a system of noninteracting Gaussian chains, eq 4.3. There are 48 chains in the oriented melt per basic cell, with one free chain in addition.

Table IV
Chain Vector Orientation and Segment Orientation for a Free Chain in Deformed Oriented Melt[a]

	λ									
	0.6	0.6	0.6	1.5	1.5	1.75	1.75	2.0	2.0	2.0
$\langle P_2\rangle_V \times 10^2$	0.3	−1.8	−1.7	1.9	7.6	1.9	4.0	8.1	7.4	7.0
$\langle P_2\rangle_S \times 10^2$	−0.6	−0.6	−0.8	1.0	1.5	1.4	2.0	2.3	2.5	2.4

[a] $N = 10$, $\mu = 48$ chains in oriented melt.

networks. Our simulations demonstrate that excluded-volume interactions as present in our model are sufficient to produce this transfer of segment orientation from the network chains to a free chain. However, in our simulations the segment orientation acquired by the free chain is much smaller than that of the oriented melt chains, whereas in the NMR results, the free chain segment orientation is equal to that of the network chain. This discrepancy may be due to the fact that our simulations employ much shorter chains than those involved in the experiments.

Chain Vector Orientation. The program also computes an orientation measure for the chain vector of the free chain immersed in the oriented melt. It is defined as

$$\langle P_2\rangle_V = \frac{1}{2}\left(\frac{3\langle R_1^2\rangle}{\langle R^2\rangle} - 1\right) \tag{4.4}$$

where R_1 is the x_1 component of the chain vector **R** and $R = |\mathbf{R}|$. The values of the chain vector orientation $\langle P_2\rangle_V$ are compared with corresponding values of the segment orientation $\langle P_2\rangle_S$ in Table IV; it is seen that the former are consistently larger than the latter. If the probability of the orientation of a given segment of the free chain were uncorrelated with the orientation of the preceding segment, as would be the case in an ideal freely jointed chain, then it is readily seen that $\langle P_2\rangle_V = \langle P_2\rangle_S$. Therefore, the present results are a consequence of the fact that, as discussed in section 3, excluded-volume effects produce some intrachain segment–segment correlation for a free chain in a dense melt (see Figure 1). We introduce the notation

$$\xi = \langle P_2\rangle_V/\langle P_2\rangle_S \tag{4.5}$$

and refer to ξ as the enhancement factor. It is used as a measure of the enhancement of the anisotropy of the chain

vector distribution that is caused by the intrachain segment–segment correlation.

$p(\mathbf{R})$ for Free Chain in Oriented Melt. The results for $\langle P_2\rangle_V$, the measure of chain vector orientation for a free chain in a deformed oriented melt, given in Table IV, show clearly that the chain vector distribution is no longer isotropic as it is in a free melt. We obtain a more detailed description of this anisotropy by sorting on the chain vector $\mathbf{R}$ of the free chain to obtain the probability density $p(\theta_V)$, where θ_V is the angle between $\mathbf{R}$ and the stretch direction. Some typical results are shown in Figure 10. Although there is substantial numerical scatter, they show clearly the tendency of a free chain in a stretched oriented melt to align its chain vector in the stretch direction.

As discussed in section 2, we may compute the chain force $\mathbf{f}$ acting on a chain with fixed chain vector in the deformed oriented melt from the probability distribution $p(\mathbf{R})$ for a free chain in the deformed oriented melt. For $p(\mathbf{R}) = p(R,\theta)$, eq 2.12 takes the form

$$f_R = -kT\frac{\partial}{\partial R}\log p(R,\theta) \tag{4.6}$$

$$f_\theta = \frac{-kT}{R}\frac{\partial}{\partial \theta}\log p(R,\theta) \tag{4.7}$$

where f_R, f_θ are the axial and transverse components of the chain force $\mathbf{f}$, Figure 8. Alternatively

$$M = -kT\frac{\partial}{\partial \theta}\log p(R,\theta) \tag{4.8}$$

where $M = Rf_\theta$ is the moment of the chain force. Since $p(R,\theta)$, as seen in Figure 10, decreases with increasing θ, f_θ is positive and the chain moment tends to turn the chain away from the stretch direction. This moment has a softening effect, in accord with the previously described simulation results, as may be seen from the following argument: Let $\mathbf{f} = \mathbf{f}_R + \mathbf{f}_\theta$ where $\mathbf{f}_R = f_R\mathbf{e}_R$, $\mathbf{f}_\theta = f_\theta\mathbf{e}_\theta$ with $\mathbf{e}_R$, $\mathbf{e}_\theta$ unit vectors in the R and θ directions, respectively. We may also express the vectors $\mathbf{f}_R$, $\mathbf{f}_\theta$ in terms of unit vectors $\mathbf{e}_i$ in the x_i directions, respectively, as $\mathbf{f}_R = f_{Ri}\mathbf{e}_i$, $\mathbf{f}_\theta = f_{\theta i}\mathbf{e}_i$ (summation over $i = 1, 2, 3$). The contribution that a typical chain makes to $t_{11} - t_{22}$ is then, from eq 1.9

$$f_1R_1 - f_2R_2 = (f_{R1} + f_{\theta 1})R_1 - (f_{R2} + f_{\theta 2})R_2 \tag{4.9}$$

Since $\mathbf{f}_\theta\cdot\mathbf{R} = f_{\theta i}R_i = 0$ and, by symmetry, $f_{\theta 2}R_2 = f_{\theta 3}R_3$

$$f_{\theta 1}R_1 = -2f_{\theta 2}R_2 \tag{4.10}$$

It therefore follows that

$$f_1R_1 - f_2R_2 = f_{R1}R_1 - f_{R2}R_2 - 3f_{\theta 2}R_2 \tag{4.11}$$

Since $f_{\theta 2}R_2 > 0$, we see that the last term represents a negative contribution to $t_{11} - t_{22}$.

Our conclusion that the anisotropy of $p(\mathbf{R})$ for a free chain in a deformed oriented melt leads to the existence of moments on the deformed chains, and that these moments have a softening effect on the stress–strain relation in uniaxial tension, makes the enhancement of the anisotropy of $p(\mathbf{R})$ by intrachain segment–segment correlation particularly important. We study this question further in the next section, using Monte Carlo methods.

5. Monte Carlo Simulations of Longer Chains

The numerical results of the preceding section support the conjecture that eq 1.5 may be used to compute the deviatoric stress (or the stress difference $t_{11} - t_{22}$ in uniaxial extension) in a system of interacting chains, providing the chain force f_i is interpreted as in section 2. The considerations of that section show that f_i can be computed in terms of the probability density $p(\mathbf{R};\lambda)$ describing a free chain in the deformed network; the notation $p(\mathbf{R};\lambda)$ emphasizes that this probability density depends on the extension λ applied to the network and that $p(\mathbf{R};\lambda)$ is anisotropic for $\lambda \neq 1$. Here we study these questions further for systems of longer chains by use of Monte Carlo techniques.

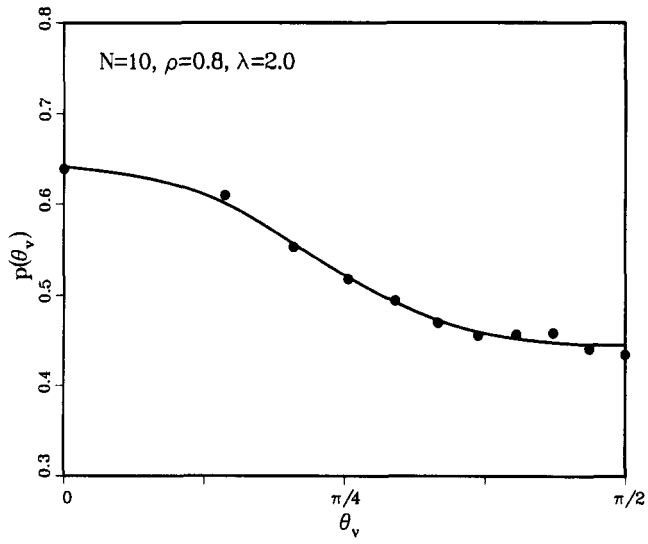

Figure 10. Probability density $p(\theta_V)$ as obtained from molecular dynamics simulation for a free chain in a stretched oriented melt (as in Figure 9), where θ_V is the angle between the chain vector $\mathbf{R}$ and the stretch direction. Values of $p(\theta_V)$ shown represent $^1/_2(p(\theta_V) + p(\pi - \theta_V))$. Curve shown drawn to aid the eye.

Chain Model. We use the rotational isomeric model for polyethylene of Jernigan and Flory[29] and employ their parameters (corresponding to $T = 413$ K) in our Monte Carlo simulations as described in ref 29. To verify our program, $\langle R^2\rangle_0$ were obtained for various N; the results were in good agreement with those of ref 29.

Enhancement Factor. The anisotropy of $p(\mathbf{R};\lambda)$ for a free chain in a deformed network is, as seen in section 4, a consequence of two separate factors: (i) the segment orientation $\langle P_2\rangle_S$ acquired by the free chain through its interactions with the chains of the deformed network and (ii) the enhanced anisotropy of the chain vector orientation $\langle P_2\rangle_V$ (see eq 4.4) that is due to intrachain segment–segment correlation.

The intrachain segment–segment correlation is, or course, already present in the rotational isomeric model. It is necessary, however, to add to the model of a single chain the desired segment orientation $\langle P_2\rangle_S$. We do this by adding to the potentials descriptive of the isolated polyethylene chain an external potential

$$V(\cos\theta_S) = -b\cos^2\theta_S \tag{5.1}$$

that acts on every segment of the chain, where θ_S is the angle between that segment and the x_1 axis. We regard this potential as replacing, in a mean-field sense, the excluded-volume interactions of the chains of the deformed network with the free chain. This mean-field approach to the study of segment orientation appears to have been initiated by Guth.[30]

Using Monte Carlo techniques we next generate a large number of sample conformations of the polyethylene model subject to $V(\cos\theta_S)$. From these we determine, by sorting, $p(\mathbf{R})$ and other quantities of interest. The results for various values of N and parameter b are given in Table V. We note that the enhancement factor ξ, defined in eq 4.4, increases with N, with $\xi \cong 4$ for $N = 500$.

Table V
Chain Vector Orientation and Segment Orientation for Rotational Isomeric State Chains

	N^a			
	50	100	200	500
$\langle P_2\rangle_V \times 10^2$	5.15	5.38	5.59	5.76
$\langle P_2\rangle_S \times 10^2$	1.38	1.40	1.43	1.45
$\xi = \langle P_2\rangle_V/\langle P_2\rangle_S$	3.74	3.84	3.91	3.97

	b/kT^b				
	0.025	0.05	0.075	0.10	0.15
$\langle P_2\rangle_V \times 10^2$	1.31	2.69	4.14	5.55	8.84
$\langle P_2\rangle_S \times 10^2$	0.35	0.70	1.06	1.42	2.19
$\xi = \langle P_2\rangle_V/\langle P_2\rangle_S$	3.74	3.84	3.90	3.91	4.03

[a] $b/kT = 0.1$ (eq 5.1). [b] $N = 200$.

Anisotropic Gaussian. For large N, the probability density $p(\mathbf{R})$ found from the Monte Carlo generation of sample conformations is found to be well fitted by an anisotropic Gaussian distribution of the form

$$p(\mathbf{R}) = C\exp\left(\frac{-R_1^2}{2q\langle R^2\rangle} - \frac{R_2^2 + R_3^2}{(1-q)\langle R^2\rangle}\right) = p_1(R_1)p_2(R_2)p_3(R_3) \quad (5.2)$$

where $q = \langle R_1^2\rangle/\langle R^2\rangle$. Examples of the fit of $p_1(R_1)$ and $p_2(R_2)$ to Gaussian distributions are shown in Figure 11.

6. Stress–Strain Relation

We now consider the stress–strain relation for a network of identical chains with fixed junctions that results from the probability distribution of eq 5.2. We use eq 1.9, which we rewrite in the form

$$t_{11} - t_{22} = \sum_{\gamma=1}^{\nu}\left(f_1(\gamma)R_1(\gamma) - \frac{1}{2}(f_2(\gamma)R_2(\gamma) + f_3(\gamma)R_3(\gamma))\right) \quad (6.1)$$

We have here set the volume of the system $v = 1$, and ν is therefore the number of chains per unit volume.

By application of eq 2.12 to eq 5.2

$$f_1 = \frac{kTR_1}{q\langle R^2\rangle} \qquad f_2 = \frac{2kTR_2}{(1-q)\langle R^2\rangle} \qquad f_3 = \frac{2kTR_3}{(1-q)\langle R^2\rangle} \quad (6.2)$$

so that

$$t_{11} - t_{22} = \frac{kT}{\langle R^2\rangle}\sum_{\gamma=1}^{\nu}\left(\frac{R_1^2(\gamma)}{q} - \frac{R_2^2(\gamma) + R_3^2(\gamma)}{1-q}\right) \quad (6.3)$$

By use of the affine assumption, eq 1.6

$$t_{11} - t_{22} = \frac{kT}{\langle R^2\rangle}\left(\sum_{\gamma=1}^{\nu}\frac{\lambda^2 R_{01}^2(\gamma)}{q} - \frac{\lambda^{-1}(R_{02}^2(\gamma) + R_{03}^2(\gamma))}{1-q}\right) \quad (6.4)$$

By the assumption of isotropy of the reference configuration in which the length of all the chain vectors is R_0

$$\sum_{\gamma=1}^{\nu}R_{01}^2 = \sum_{\gamma=1}^{\nu}R_{02}^2 = \sum_{\gamma=1}^{\nu}R_{03}^2 = \nu R_0^2/3 \quad (6.5)$$

and eq 6.4 becomes

$$t_{11} - t_{22} = \frac{\nu kT}{3}\left(\frac{R_0^2}{\langle R^2\rangle}\right)\left(\frac{\lambda^2}{q} - \frac{2\lambda^{-1}}{1-q}\right) \quad (6.6)$$

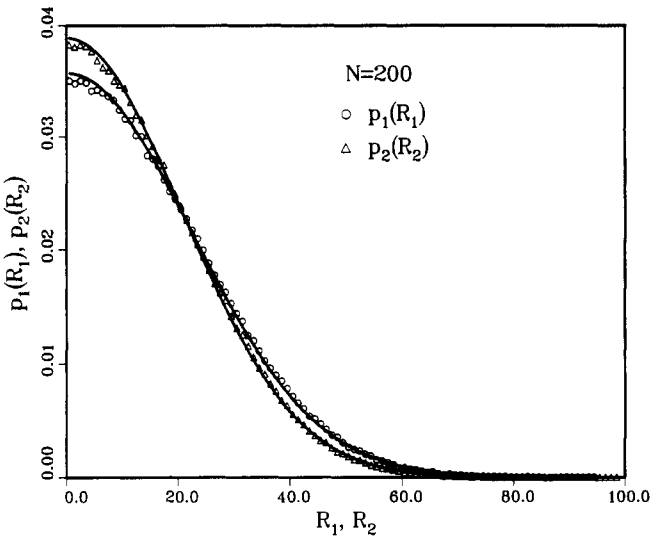

Figure 11. Probability densities $p_1(R_1)$ and $p_2(R_2)$ as obtained from Monte Carlo simulations of rotational isomeric state chains with added potential, eq 5.1, to produce segment orientation with respect to x_1 axis. Solid curves are Gaussian curves corresponding to computed values of $\langle R_1^2\rangle$ and $\langle R_2^2\rangle$. The parameter $b/kT = 0.1$ in eq 5.1.

Note that in the special case of an isotropic Gaussian, $q = {}^1/_3$ and eq 6.6 becomes equivalent to eq 1.7.

We next introduce the chain vector orientation $\langle P_2\rangle_V$ which we here abbreviate to P_2, so that

$$P_2 = \frac{1}{2}(3q - 1) \quad (6.7)$$

and

$$t_{11} - t_{22} = \nu kT\left(\frac{R_0^2}{\langle R^2\rangle}\right)\left(\frac{\lambda^2}{1+2P_2} - \frac{\lambda^{-1}}{1-P_2}\right) \quad (6.8)$$

or

$$t_{11} - t_{22} = \nu kT\left(\frac{R_0^2}{\langle R^2\rangle}\right)(\lambda^2 - \lambda^{-1})\left(1 - 2P_2 - \frac{3P_2}{\lambda^3 - 1}\right) \quad (6.9)$$

where, in eq 6.9, we have assumed $P_2 \ll 1$.

Thus far we have made no assumptions regarding the dependence of the parameters of $p(\mathbf{R})$, eq 5.2, on the extension ratio. From the results of our simulations it appears reasonable to assume that $\langle R^2\rangle$ is independent of λ, and we denote this constant value by $\langle R^2\rangle_0$. Furthermore, we take $R_0^2 = \langle R^2\rangle_0$. As far as q, or equivalently P_2, is concerned, we assume first that the segment orientation $\langle P_2\rangle_S$ obeys a relation of the form

$$\langle P_2\rangle_S = \beta(\lambda^2 - \lambda^{-1}) \quad (6.10)$$

with β a constant. This is the known form of the relation for a system of noninteracting Gaussian chains, eq 4.3, and has been observed to apply, as well, for a free chain interacting with a deformed network.[21] Furthermore, on the basis of the developments in sections 4 and 5, we assume that

$$P_2 = \xi\langle P_2\rangle_S = \xi\beta(\lambda^2 - \lambda^{-1}) \quad (6.11)$$

where the enhancement factor ξ is also taken as constant. (In our simulations we see a small dependence ($\sim$5%) of ξ on the parameter b that determines segment orientation (eq 5.1); in the interest of simplicity this variation is neglected.) With these assumptions eq 6.9 assumes the form

$$t_{11} - t_{22} = \nu kT(\lambda^2 - \lambda^{-1})(1 - \xi\beta(2\lambda^2 + \lambda^{-1})) \quad (6.12)$$

We can also make the assumption, as in the derivation of eq 1.10, that $t_{22} = 0$ and rewrite eq 6.12 in terms of $T_{11} = \lambda^{-1}t_{11}$ to obtain

$$T_{11} = \nu kT(\lambda - \lambda^{-2})(1 - \xi\beta(2\lambda^2 + \lambda^{-1})) \qquad (6.13)$$

For numerical evaluation, we use the value $\beta = 0.0014$ taken from the experimental results of Sotta et al.[21] and $\xi = 4$ based on the Monte Carlo results of section 5. The result is shown in Figure 12. It is seen that eq 6.13 predicts a softening of approximately 10% at $\lambda = 3$.

Thermodynamic Consideration. We next relate the force-based expression for the stress difference, eq 1.9, to that obtained from thermodynamic considerations. From the principles of continuum mechanics and thermodynamics applied to a system that is isotropic in its reference configuration[31]

$$v(t_{11} - t_{22}) = \lambda_1 \frac{\partial F}{\partial \lambda_1} - \lambda_2 \frac{\partial F}{\partial \lambda_2} \qquad (6.14)$$

where $F(\lambda_1,\lambda_2,\lambda_3,T)$ is the Helmholtz free energy of the system and λ_i, are the extensions in the three principal directions, x_i, $i = 1, 2, 3$.

If we assume that the chains of the system are noninteracting, we can write

$$F(\lambda_1,\lambda_2,\lambda_3,T) = \sum_{\gamma=1}^{\nu} F^*(\mathbf{R}(\gamma),T) \qquad (6.15)$$

where $F^*(\mathbf{R},T)$ is the free energy of a single chain with end-to-end vector $\mathbf{R}$. The dependence on λ_i of the right-hand side of eq 6.15 arises from the assumed affine relation between $\mathbf{R}(\gamma)$ and $\mathbf{R}_0(\gamma)$

$$R_i = \lambda_i R_{0i} \qquad (6.16)$$

We therefore find that

$$\begin{aligned} v(t_{11} - t_{22}) &= \sum_{\gamma=1}^{\nu}\left[\lambda_1 \frac{\partial F^*}{\partial R_1}R_{01} - \lambda_2 \frac{\partial F^*}{\partial R_2}R_{02}\right] \\ &= \sum_{\gamma=1}^{\nu}\left[\frac{\partial F^*}{\partial R_1}R_1 - \frac{\partial F^*}{\partial R_2}R_2\right] \\ &= \sum_{\gamma=1}^{\nu}[f_1(\gamma)R_1(\gamma) - f_2(\gamma)R_2(\gamma)] \end{aligned} \qquad (6.17)$$

where, in the last step, we have used the relation

$$f_i = \partial F^*/\partial R_i \qquad (6.18)$$

that follows from eq 2.4 and the relation $F^*(\mathbf{R},T) = -kT \log Z(\mathbf{R},T)$. We have therefore demonstrated the equivalence of the force-based expression for the stress difference with that based on thermodynamic considerations for systems of noninteracting chains.

To what extent does this equivalence apply in the presence of chain–chain interaction? In this case we have seen that $p(\mathbf{R}) = p(\mathbf{R};\lambda)$; that is, the probability density describing a free chain in a deformed network depends on the extension λ applied to the network, since λ determines the anisotropy of the network and of $p(\mathbf{R})$. The same applies as well, therefore, to $F^*(\mathbf{R},T) = F^*(\mathbf{R},T;\lambda)$. If we apply eq 6.15 to a system of interacting chains, the deformation parameters, λ_i, appear in $F(\lambda_1,\lambda_2,\lambda_3,T)$ for two reasons: through the affine deformation of $\mathbf{R}(\gamma)$ and through the anisotropy effect on $p(\mathbf{R})$. It is clear from the above derivation that equivalence between the thermodynamic approach and the force-based stress formula will remain valid providing that only the dependence on λ arising directly from the affine deformation is considered when the differentiations in eq 6.14 are performed. If, however, the two sources of λ dependence in F^* are lumped together before differentiation, the resulting stress will not be equivalent to the result obtained from the force-based expression. Note that the point at question here is not that of the validity of eq 6.14; rather it is the possibility of obtaining $F(\lambda_1,\lambda_2,\lambda_3,T)$ by simply adding the free energy of the individual chains, as in eq 6.15, when chain–chain interactions are present.

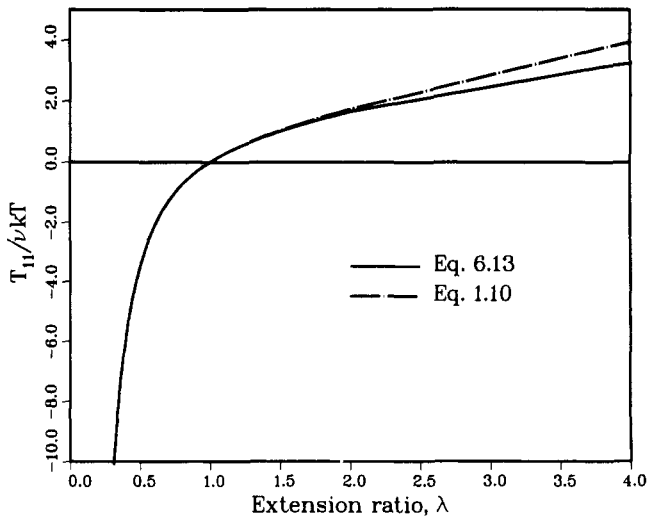

Figure 12. Comparison of stress–strain relation as computed on the basis of the anisotropic Gaussian theory, eq 6.13, with the classical molecular theory, eq 1.10, with $[R_0^2/\langle R^2\rangle_0] = 1$. The chain vector anisotropy enhancement factor $\xi = 4$, based on our Monte Carlo simulations, and the parameter $\beta = 0.0014$, based on experimental data of Sotta et al.[21]

7. Summary and Conclusion

In previous work we have considered the nature of stress in rubberlike solids on the atomic level. These solids generally exhibit negligible change in volume in deformation such as uniaxial extension and are treated as incompressible. As a result, attention is confined only to the deviatoric stress, that is the difference between the total stress tensor and the mean stress. We have used the virial formula that expresses the stress in terms of time-averaged atom–atom interactions. At the liquidlike densities appropriate to these materials, we found that the deviatoric stress is primarily due to the noncovalent excluded-volume interactions. This physical picture appears to be quite different from the classical one in which the deviatoric stress is ascribed solely to the tensile forces exerted by the chains acting as entropic springs.

In the present paper we have attempted to reconcile the two viewpoints by developing a molecular description of stress in terms of chain forces, using a definition of the chain force that keeps covalent and noncovalent interactions on an equal footing. This definition is based on the consideration of a chain with fixed end-to-end vector $\mathbf{R}$, termed a tethered chain, in interaction with a dense collection of other chains. Let the fixed end atoms of the tethered chain be at $\mathbf{x}_0$ and $\mathbf{x}_N$ with $\mathbf{x}_N - \mathbf{x}_0 = \mathbf{R}$. We define the chain force $\mathbf{f}$ as the negative of the time-averaged resultant of all forces, covalent and noncovalent, intrachain and interchain, exerted on atom N of the tethered chain by the remaining atoms of the system.

The principal results we have obtained using this definition of chain force are as follows:

(1) A virial expression for the chain force has been derived, eq 2.10, that expresses $\mathbf{f}$ in terms of the forces exerted on all of the atoms of the chain.

(2) The chain force **f** for a tethered chain with fixed chain vector **R** in interaction with a given environment can also be computed, by use of eq 2.12, from the probability density $p(\mathbf{R})$ that describes the chain vector distribution for a free chain in the same environment.

(3) When the environment of the tethered chain is a free melt of like chains, then, for sufficiently high reduced density ρ and sufficiently long chains, the simulation results show that the probability density $p(\mathbf{R})$ for the corresponding free chain approaches the Gaussian form. This is in accord with the Flory theorem. The chain force values obtained from this $p(\mathbf{R})$ are in good agreement with those obtained from the simulation of the tethered chain and the direct computation from this simulation of the chain force **f**. However, the direct computation of **f** permits its decomposition into covalent, intramolecular, and intermolecular noncovalent contributions. In the absence of noncovalent interactions there are only the covalent interactions that *pull* the end atoms inward. This is the usual entropic spring picture. However, in the presence of noncovalent excluded-volume interactions, our simulations show that, primarily, the end atoms are *pushed* inward by the intermolecular excluded-volume interactions; these latter interactions have an asymmetrical effect on the chain end atoms because they are screened by the other atoms of the tethered chain.

This finding that the chain force at liquidlike densities arises primarily from the screened noncovalent excluded-volume interaction is the counterpart, on the molecular level, to our previous conclusions regarding the primary contribution made by these interactions on the atomic level to the deviatoric stress in a deformed network.

(4) The general considerations discussed in (1) and (2) apply as well to the case of a tethered chain in an environment that consists of a deformed network or, as in this paper, an oriented melt model of a deformed network. However, in this case, the probability density for the corresponding free chain in an anisotropic environment becomes itself anisotropic and takes the form $p(\mathbf{R};\lambda)$; since the degree of anisotropy of the environment depends on its state of deformation, characterized here by the extension ratio λ, the same is the case for the probability density.

An important consequence of the anisotropy of $p(\mathbf{R};\lambda)$ is that the resulting chain force, obtained by application of eq 2.12, is no longer axial—that is, it is no longer directed along the chain vector **R**. Equivalently we may describe the result of $p(\mathbf{R};\lambda)$ as consisting of an axial force plus an applied moment, eq 4.7 and Figure 8. In the case of uniaxial extension, this moment tends to turn the chain away from the stretch direction.

(5) In the classical molecular theory the noncovalent excluded-volume interactions are assumed to make only an isotropic or hydrostatic contribution to the stress. The deviatoric stress in that theory is due solely to the tensile entropic chain force and can be computed in terms of the force-based stress formula, eq 1.5. In the present work we have seen that the excluded-volume interactions are, in fact, primarily responsible for the chain force. We have conjectured that the force-based stress formula, eq 1.5, can still be employed to compute the deviatoric stress with the chain force so defined. In other words, we assume that the excluded-volume interaction makes an anisotropic contribution to the stress only through its contribution to the chain force and that any other excluded-volume contribution to the stress is isotropic. Our simulation results in which we compute the stress in an oriented melt model for a deformed network both by means of the rigorous atomic virial formula and by the force-based formula fully support the validity of this conjecture.

(6) Analysis by means of the force-based formula of the stress difference $t_{11} - t_{22}$ in an oriented melt subjected to uniaxial extension λ shows that the nonaxiality of the chain force due to the anisotropy of $p(\mathbf{R};\lambda)$ has a softening effect; i.e., it causes $t_{11} - t_{22}$ to be smaller than it would be if only the axial component of the chain force were used in the force-based formula.

(7) A stretched oriented melt develops, as expected, preferred segment orientation as measured by $\langle P_2(\cos\theta_S)\rangle = \langle P_2\rangle_S$ where θ_S is the angle between the segment and the stretch direction. When a completely free chain is immersed in this stretched system of chains, the simulations show that the segments of the free chain acquire comparable segment orientation. These simulation results are in agreement with the H^2 NMR results of Sotta et al.[21] and show that the excluded-volume interactions present in our model are sufficient to transfer the segment orientation from the stretched system of chains to the free chain.

The segment orientation acquired by the free chain may be regarded as the mechanism responsible for the anisotropic character of $p(\mathbf{R};\lambda)$. However, it is found that the anisotropy of $p(\mathbf{R};\lambda)$ is greater than that of the individual segment distribution. More specifically, a chain vector orientation measure $\langle P_2\rangle_V$ may be defined, eq 4.4, in a manner analogous to the definition of $\langle P_2\rangle_S$, eq 4.2; it is then found from the simulations that $\langle P_2\rangle_V > \langle P_2\rangle_S$. This enhancement of anisotropy is due to the intrachain segment–segment correlation that is present in our freely jointed chain model due to excluded-volume interactions.

(8) The simulations described thus far have been performed by molecular dynamics for dense systems of interacting chains. With this approach it has not been possible to get accurate results of the type reported here for chains with more than $N = 30$ bonds. To explore the nature of the enhancement factor $\xi = \langle P_2\rangle_V/\langle P_2\rangle_S$ for longer chains we performed Monte Carlo simulations of a single chain using the polyethylene model of Jernigan and Flory.[29] Intrachain segment–segment correlation is, of course, already present in the model by virtue of the valence angle restriction and the rotational potentials. To produce segment orientation with respect to a fixed direction in space representing the stretch direction, an additional potential, eq 5.1, is added. The Monte Carlo results give an enhancement factor $\xi \cong 4$ for $N = 500$. They also show that $p(\mathbf{R};\lambda)$ is well described in terms of an anisotropic Gaussian distribution.

(9) An analytical expression for $t_{11} - t_{22}$ based on an anisotropic Gaussian expression for $p(\mathbf{R};\lambda)$ and the force-based formula has been derived. It contains two additional parameters beyond those found in the classical theory; a parameter β describing the segment orientation proportionality to $(\lambda^2 - \lambda^{-1})$ and ξ, the anisotropy enhancement factor. If we use, for illustrative purposes, $\xi = 4$ based on the MC simulations and the value of $\beta = 0.0014$ based on the ^2H NMR results of Sotta et al.,[21] we find a softening relative to the classical theory of $\sim 10\%$ at $\lambda = 3$.

Relationship to Other Work. Our work has dealt with clarification of the role of excluded volume in the chain force concept as well as the effect of excluded volume on segment orientation and its consequent effect on the stress–strain relation. While the first question does not appear to have been studied previously, the second has received considerable attention. The earliest analysis of excluded-volume effects on the stress–strain relation of rubber elasticity is due to DiMarzio,[16] who employed a lattice

model to evaluate the additional packing entropy due to the competition of chains for space. Other early treatments of this aspect of the theory were given by Jackson, Shen, and McQuarrie[17] and by Tanaka and Allen.[18] In particular, the analysis of Jackson et al.[17] is closest in spirit to ours, since they employ an anisotropic Gaussian to describe what we have termed $p(\mathbf{R};\lambda)$. The subject of the role of segment orientation continues to be an active research area today.[32-35] In addition to theoretical studies, an important new development is the use of ^{2}H NMR to measure segment orientation in deformed networks.[20,21] The experimental results obtained in this way for the segment orientation acquired by a free chain in a deformed network are of particular interest since, as we have seen, this is precisely the type of information needed in the calculation of $p(\mathbf{R};\lambda)$. Further results that would explore the effect of chain length on segment orientation would be valuable, while a method for the measurement of chain vector orientation would permit experimental investigation of the enhancement factor.

Although the theoretical treatments take various routes, they generally arrive at the conclusion that the enhanced segment orientation due to excluded-volume interactions results in a softening, with respect to the classical result, in the stress–strain relation. However, most of the analyses arrive at the conclusion that the magnitude of the predicted softening is too small to qualify this excluded-volume effect as the sole or principal cause of the observed Mooney effect. The present analysis introduces a new concept, the enhancement factor ξ, that acts as a multiplier of the expected softening. With the value $\xi \cong 4$ obtained from Monte Carlo studies our results indicate that this mechanism can, in fact, represent a substantial contribution to the Mooney effect, although the magnitude of the effect we obtain is still too small to qualify it as its sole cause.

Acknowledgment. This work has been supported by the Gas Research Institute (Contract 5085-260-1152). The computations were performed on the Cray Y-MP at the Pittsburgh Supercomputing Center.

References and Notes

(1) See, for example: Jongschaap, R. J. J. *Rep. Prog. Phys.* **1990**, *53*, 1–55; in particular, see eq 3.7, p 19.
(2) Gao, J.; Weiner, J. H. *Macromolecules* **1989**, *22*, 979.
(3) Gao, J.; Weiner, J. H. *J. Chem. Phys.* **1989**, *90*, 6749.
(4) Weiner, J. H.; Gao, J. In *Molecular Basis of Polymer Networks*; Baumgartner, A., Picot, C. E., Eds.; Springer Proceedings in Physics 42; Springer: Berlin, 1989; pp 184–188.
(5) Gao, J.; Weiner, J. H. *Macromolecules* **1991**, *24*, 1519.
(6) Ronca, G.; Allegra, G. J. *J. Chem. Phys.* **1975**, *63*, 4990.
(7) See, for example, the discussion in: Mark, J. E.; Erman, B. *Rubberlike Elasticity. A Molecular Primer*; Wiley-Interscience: New York, 1988; p 12.
(8) de Gennes, P.-G. *Scaling Concepts in Polymer Physics*; Cornell University: Ithaca, NY, 1979; p 54.
(9) Flory, P. J. *J. Chem. Phys.* **1949**, *17*, 303.
(10) Edwards, S. F. *J. Phys.* **1975**, *A8*, 1670.
(11) Doi, M.; Edwards, S. F. *The Theory of Polymer Dynamics*; Clarendon Press: Oxford, U.K., 1986; pp 149–151.
(12) Curro, J. G. *J. Chem. Phys.* **1974**, *61*, 1203.
(13) Gao, J.; Weiner, J. H. *Macromolecules* **1987**, *20*, 2525.
(14) Kremer, K.; Grest, G. S. *J. Chem. Phys.* **1990**, *92*, 5057.
(15) Richards, R. W.; Maconnachie, A.; Allen, G. *Polymer* **1978**, *19*, 266.
(16) DiMarzio, E. A. *J. Chem. Phys.* **1962**, *36*, 1563.
(17) Jackson, J. L.; Shen, M. C.; McQuarrie, D. A. *J. Chem. Phys.* **1966**, *44*, 2388.
(18) Tanaka, T.; Allen, G. *Macromolecules* **1977**, *10*, 426.
(19) Gao, J.; Weiner, J. H. *Macromolecules* **1988**, *21*, 773.
(20) Gronski, W.; Stadler, R.; Jacobi, M. M. *Macromolecules* **1985**, *17*, 741.
(21) Sotta, P.; Deloche, B.; Herz, J.; Lapp, A.; Durand, D.; Rabadeux, J.-C. *Macromolecules* **1987**, *20*, 2769. See also: Deloche, B.; Sotta, P. *Recherche* **1989**, *20*, 958.
(22) See, for example: Weiner, J. H. *Statistical Mechanics of Elasticity*; John Wiley: New York, 1986; pp 228–231.
(23) Gao, J.; Weiner, J. H. *Macromolecules* **1987**, *20*, 2520.
(24) Reference 22, pp 235–236.
(25) Flory, P. J. *Statistical Mechanics of Chain Molecules*; Interscience: New York, 1969; p 11.
(26) The representation of the covalent bond used by Kremer and Grest[14] is somewhat softer than ours.
(27) This is not the case for sufficiently small values of R/Na and low reduced density ρ; see Figure 2 of ref 13.
(28) Kuhn, W.; Grun, F. *Kolloid-Z.* **1942**, *101*, 248.
(29) Jernigan, R. L.; Flory, P. J. *J. Chem. Phys.* **1969**, *50*, 4165.
(30) Guth, E. *J. Polym. Sci., Part C* **1966**, *12*, 89.
(31) See, for example: Ogden, R. W. *Rubber Chem. Technol.* **1986**, *59*, 361.
(32) Jarry, J.-P.; Monnerie, L. *Macromolecules* **1979**, *12*, 316.
(33) Deloche, B.; Samulski, E. T. *Macromolecules* **1988**, *21*, 3107.
(34) Walasek, J. *J. Polym. Sci., Part B* **1990**, *28*, 2473.
(35) Erman, B.; Bahar, I.; Kloczkowski, A.; Mark, J. E. *Macromolecules* **1990**, *23*, 5335.